Nature Environment and Pollution Technology
An International Quarterly Scientific Journal

p-ISSN: 0972-6268
(Print copies up to 2016)
e-ISSN: 2395-3454

Vol. 21 | No. 1 | pp. 263-268 | 2022

Original Research Paper

https://doi.org/10.46488/NEPT.2022.v21i01.030

Open Access Journal

Mechanism and Chemical Stability of U(VI) Removal by Magnetic Fe_3O_4 @Biochar Composites

Erhui Zhao*, Anjie Wang*, Luojia Huang, Chengguang Chen** and Muqing Qiu*†**

*School of Life Science, Shaoxing University, Shaoxing, 312000, P. R. China

**School of Architectural Engineering, Shaoxing University Yuanpei College, Shaoxing, 312000, P. R. China

†Corresponding author: Muqing Qiu; qiumuqing@126.com

Nat. Env. & Poll. Tech.
Website: www.neptjournal.com

Received: 16-04-2021
Revised: 13-05-2021
Accepted: 08-06-2021

Key Words:
Magnetic Fe_3O_4@Biochar
U(VI)
Chemical stability
Radioactive wastewater

ABSTRACT

Biochar is typically made via pyrolysis of organic materials under anoxic conditions, due to its high surface area and significant negative charge. It also has the ability to minimize the mass or volume of waste items. As a result, biochar is frequently used in the remediation of environmental contamination. To overcome the shortcoming of biochar in the application, the magnetic Fe_3O_4@Biochar from walnut shells were prepared. The magnetic Fe_3O_4@Biochar from walnut shells is used to study the adsorption of U(VI) in the solution. SEM, XRD, and FT-IR are used to determine the properties of magnetic Fe_3O_4@Biochar. The results revealed that magnetic Fe_3O_4@Biochar has a fragmented and irregular form. On the surface of magnetic Fe_3O_4@Biochar, several functional groups can aid in the adsorption of pollutants. The adsorption capacity of U(VI) by magnetic Fe_3O_4@Biochar is influenced by the contact time and initial concentration of U(VI). For the adsorption of U(VI) in solution by magnetic Fe_3O_4@ Biochar, the pseudo-first-order kinetic equation and the Langmuir isotherm equation can be fitted. The adsorption of the process is chemical adsorption and monolayer adsorption. The chemical stability of magnetic Fe_3O_4@Biochar is very well.

INTRODUCTION

Uranium is a heavy metal element with radioactivity and high toxicity, which poses a great threat to the ecological environment and human health (Dong et al. 2017, Qiu et al. 2021). During the various stages of nuclear power plants and nuclear accidents, a certain amount of uranium-containing radioactive wastewater will be generated (Vogel et al. 2010, Qiu et al. 2018, Hu et al. 2021). Therefore, the uranium-containing radioactive wastewater must be treated. Physical or physical-chemical approaches are used in the majority of traditional radioactive wastewater treatment procedures. Chemical precipitation, evaporation, ion exchange, and membrane separation are commonly used to treat low and medium concentrations of radioactive wastewater (Bhat et al. 2008, Qiu & Huang 2017, Hao et al. 2021, Liu et al. 2021).

In most circumstances, traditional radioactive wastewater treatment methods have a high removal efficiency. However, several issues remain, such as high chemical consumption, high energy consumption, rapid corrosion and scaling, and secondary pollution (Febrianto et al. 2009, Das 2012, Wang et al. 2021). The adsorption method has gradually attracted people's attention due to its characteristics of high efficiency, energy saving, environmental protection, and recyclability.

Because of the high surface area and considerable negative charge, biochar is ordinarily fabricated by the pyrolysis of organic materials under anoxic conditions (Zhang et al. 2013, Li et al. 2019, Dai et al. 2021). Moreover, it can also reduce the mass or volume of waste materials (Han et al. 2016, Yao et al. 2021). Therefore, biochar is applied to the remediation of environmental pollution widely (Qiu and Huang 2017, Jang et al. 2018, Mohanty et al. 2018, Wang et al. 2020). The spectrum of raw materials available to identify affordable biochar resources has been expanding in recent years (Sun et al. 2015, Dutta & Nath 2018, Li et al. 2019). Agricultural by-products and industrial waste, such as peanut shells, straws, walnut shells, and so on, are available in addition to standard high-quality wood and wood chips (Xu et al. 2014, Chang et al. 2017, Wang et al. 2018). The annual output of walnuts in China is more than 200,000 tons, and its shell and outer peel are almost discarded as waste. A large number of walnut shells were burned, causing great waste of resources and air pollution. Therefore, biochar is applied to the remediation of environmental pollution widely, such as heavy metals, organic pollution, and inorganic pollution (Chen et al. 2021). Biochar, on the other hand, is difficult to recycle in the application. As a result, magnetic biochar may be readily recycled, reused, and costs can be lowered.

Therefore, in this study, walnut shells are used as raw materials to prepare biochar. The main objectives are: 1) the magnetic Fe_3O_4@Biochar is synthesized; 2) the characteristics of magnetic Fe_3O_4@Biochar are discussed in

detail according to the results of SEM, EDS, XRD, and FT-IR; 3) the adsorption experiments are also carried out; 4) the adsorption mechanism is elaborated according to adsorption kinetics and adsorption isotherm. This study is of great significance for new sources of biochar raw materials. It provides a new way for the resource utilization of crop wastes.

MATERIALS AND METHODS

Materials

Walnut shells are obtained from a farm in the City of Linan, Zhejiang Province, P.R. China. Biochar was prepared using walnut shells. The walnut shells were washed three times with water and dried at 378 K to a consistent weight. Then they were pulverized and passed through a 20 meshes sieve. At a temperature of 523 K, 10 g of walnut shell is pyrolyzed for 2 h in a nitrogen atmosphere. It was pulverized through 100 meshes after cooling to room temperature. Then, the biochar from walnut shells is obtained.

1 g of biochar was added to 250 mL Erlenmeyer flask. Then, we added 100 mL of 1 mol.L^{-1} Fe^{-3+} and stirred for 30 min under ultrasonic conditions. Finally, we added 100 mL of 3 mol.L^{-1} NaOH solution and stirred for 60 min under ultrasonic conditions. They were washed with DMF until the supernatant was clear. Then, they were dried under vacuum at 80° for 12 h. The magnetic Fe_3O_4@Biochar was obtained for adsorption experiments.

Adsorption Experiment

Adsorption tests were carried out in a set of 250 mL Erlenmeyer flasks containing magnetic Fe_3O_4@Biochar and 100 mL U(VI), with initial concentrations in an aqueous solution. The flasks were shaken at 303 K and 150 rpm at a steady temperature. After that, the samples were filtered, and the residual U(V) concentration was determined.

Analytical Methods

The concentration of U(VI) ion in solution was measured with a UV-1600 spectrophotometer. The adsorption capacity of U(VI) and removal rate of U(VI) were calculated as follows:

$$q_e = \frac{(C_0 - C_e) \times V}{m} \quad \ldots(1)$$

$$R = \frac{C_e}{C_0} \times 100\% \quad \ldots(2)$$

Where, C_0 and C_e (mg.L^{-1}) are the initial and equilibrium concentrations of U(VI) in solution respectively. q_s (mg.g^{-1}) is the adsorption amount per unit mass of the biochar at adsorption equilibrium. V (mL) is the volume of solution, m(g) is the mass of the biochar. R(%) is the removal rate of U(VI) ions in an aqueous solution.

SEM (Ultra 55), X-ray diffraction (Ulitma IV), and Fourier transform infrared spectroscopy spectra (Nicolet 5700) were used to study the physicochemical features of the magnetic Fe_3O_4@Biochar made from walnut shells.

RESULTS AND DISCUSSION

The Characteristic of the Magnetic Fe_3O_4@Biochar from Walnut Shells

Fig.1 (A and B) shows the SEM images of biochar and the magnetic Fe_3O_4@Biochar. It suggests that the shape of biochar and the magnetic Fe_3O_4@Biochar are fragmented and irregular. They have no pore structure. The irregular structure is an advantage for the adsorption of U(VI) ions in the solution. Additionally, as shown from Fig. 1B, a lot of small particles can be observed on the surface of magnetic Fe_3O_4@Biochar. It indicates that Fe_3O_4 nanoparticles are loaded successfully. This result can be verified by the EDS (Fig. 2). As shown from Fig. 2A and 2B, the elements of C, O, K and Mg appeared on the surface of biochar. After

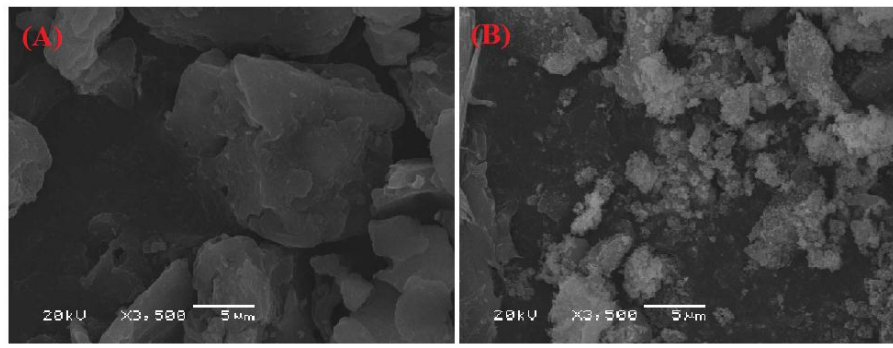

Fig.1: SEM image of biochar (A) and the magnetic Fe_3O_4@Biochar (B).

preparation, the element of Fe can be determined on the surface of the magnetic Fe_3O_4@Biochar.

The possible function groups of the magnetic Fe_3O_4@Biochar are observed by FT-IR (Fig. 3A). There are seven peaks on the magnetic Fe_3O_4@Biochar. They are 3358, 2332, 1608, 1377, 1059, 569 and 405 cm^{-1}, respectively. They are assigned as -O-H, -C≡C-, -C=C-, -C-H, -C-C, and -C-H, respectively. It suggests that there are a large number of functional groups on the surface of the magnetic Fe_3O_4@Biochar, which can facilitate the adsorption of pollutants. The results of the XRD pattern are shown in Fig. 3B. The characteristic peak of the magnetic Fe_3O_4@Biochar can be observed. It is 21.35°. This result corresponds to previous studies.

Adsorption Experiment

Adsorption experiments are conducted in a set of 250 mL Erlenmeyer flasks. First, the effect of contact time on adsorption capacity is tested. Experimental conditions are followings: C_0 = 60 $mg.L^{-1}$, pH = 4.31, Temperature 308 K, rotating speed = 150 rpm, dosage of the magnetic Fe_3O_4@Biochar is 0.4 g. The results of the experiment are shown in Fig. 4A and 4B.

At the first stage of adsorption, the adsorption rate increases quickly. It may be the reason that there are a large number of adsorption sites on the surface of the magnetic Fe_3O_4@Biochar. Therefore, the adsorption rate increases very quickly. After 30 min, as the contact time increases, the adsorption rate increases slowly. It may be the reason that the adsorption sites on the surface of the magnetic Fe_3O_4@Biochar begin to decrease. As the adsorption time continues to increase, adsorption gradually reaches adsorption equilibrium. The influence of initial solution concentration U(VI) on adsorption capacity is then tested. Experimental conditions are followings: contact time 360 min, pH = 4.31, Temperature 308 K, rotating speed = 150 rpm, the dosage of the magnetic Fe_3O_4@Biochar is 0.1 g. The results of the experiment are shown in Fig. 4B. As the adsorption time increases, the adsorption capacity gradually decreases. When the initial concentration of U(VI) in solution is 100 $mg.L^{-1}$, the adsorption capacity of U(VI) by the magnetic Fe_3O_4@Biochar reaches 4.71 $mg.g^{-1}$.

Adsorption Kinetics

To describe the adsorption kinetic of U(VI) in solution by the magnetic Fe_3O_4@Biochar, pseudo-first-order kinetic equation and pseudo-second-order kinetic equation are used in this study. Their equations are as follows (Mellah et al. 2006, Troyer et al. 2016):

$$q_t = q_e(1 - e^{-K_1 t}) \quad \ldots(3)$$

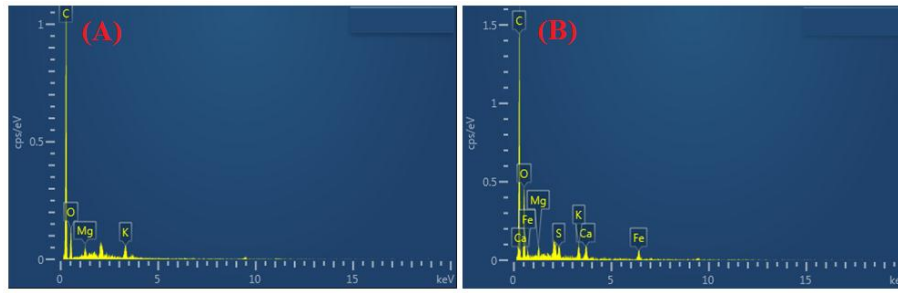

Fig. 2: EDS of biochar (A) and the magnetic Fe_3O_4@Biochar (B).

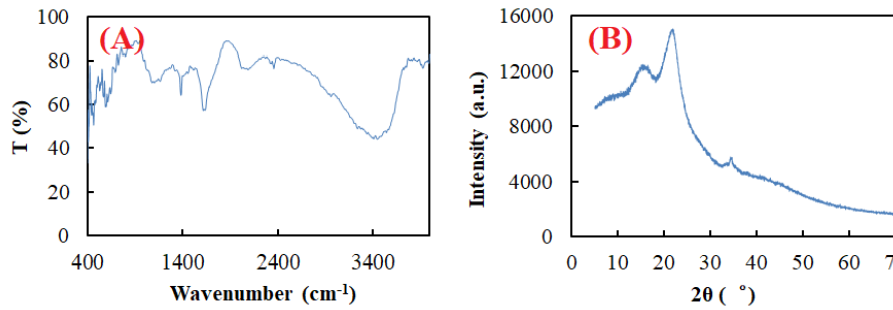

Fig. 3: FT-IR spectra (A) and XRD pattern (B) of the magnetic Fe_3O_4@Biochar.

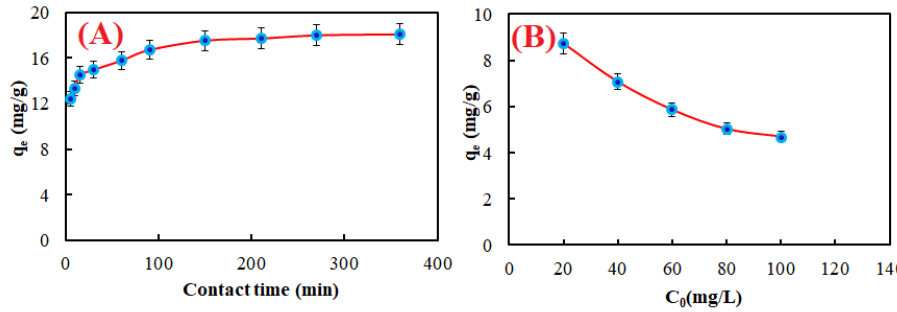

Fig. 4: Effect of contact time (A) and initial concentration of U(VI) (B) on adsorption capacity by the magnetic Fe_3O_4@Biochar.

$$\frac{t}{q_t} = \frac{1}{K_2 q_e^2} + \frac{t}{q_e} \quad \ldots(4)$$

Where q_t (mg.g^{-1}) and q_s (mg.g^{-1}) are adsorption capacity of U(VI) in solution by the magnetic Fe_3O_4@Biochar at adsorption time t and adsorption equilibrium respectively. K_1 (min^{-1}) and K_2 (min^{-1}) are the adsorption rate constants.

The adsorption kinetic equation of U(VI) ion by the magnetic Fe_3O_4@Biochar from walnut shells is shown in Fig. 5A and 5B. As shown in Fig. 5A and 5B, it can be concluded that the adsorption process can be ascribed with a pseudo-second-order kinetic equation (R^2 = 0.9997). It indicates that the adsorption process of U(VI) in solution by the magnetic Fe_3O_4@Biochar is chemical adsorption. Chemical adsorption is the most common form of adsorption.

Adsorption Isotherms

To describe the adsorption isotherm of U(VI) ion by the magnetic Fe_3O_4@Biochar, Langmuir isotherm equation and Freundlich isotherm equation are applied in this study. Their equations are follows (Freundlich 1906, Langmuir 1918):

$$\frac{c_e}{q_e} = \frac{c_e}{q_{max}\frac{1}{K_L q_{max}}} \quad \ldots(5)$$

$$lg\, q_e = lg\, K_F + \frac{1}{n} lg\, c_e \quad \ldots(6)$$

Where q_e (mg.g^{-1}) is the adsorption capacity of U(VI) in solution by the magnetic Fe_3O_4@Biochar at adsorption equilibrium. q_{max} (mg.g^{-1}) is the maximum adsorption capacity of the adsorbent under specific adsorption conditions. K_L (L.mg^{-1}) and K_F (L.mg^{-1}) are the adsorption rate constants. C_S (mg.L^{-1}) is equilibrium concentrations of U(VI) in solution.

The adsorption isotherm of U(VI) ion by the magnetic Fe_3O_4@Biochar from walnut shells is shown in Fig. 6. According to the value of R^2, it can be suggested that Langmuir isotherm is more suitable for the adsorption of U(VI) ions in solution by the magnetic Fe_3O_4@Biochar. The adsorption process is the adsorption of the monolayer.

Stability of Adsorption U(VI) Ions in Aqueous Solution

100 mL of 0.1 mol.L^{-1} NaOH and 100 mL of 0.01 mol.L^{-1} HCl were used to rinse the magnetic Fe_3O_4@Biochar. Then it's washed again with distilled water for 5 min. The magnetic Fe_3O_4@Biochar prepared in this way is used as adsorbents in recycling experiments. The repeated reusability of the magnetic Fe_3O_4@Biochar is displayed in Fig.7. It shows that the removal rate of U(VI) decreases from 65.56% to 49.14% during five adsorption and desorption experiments.

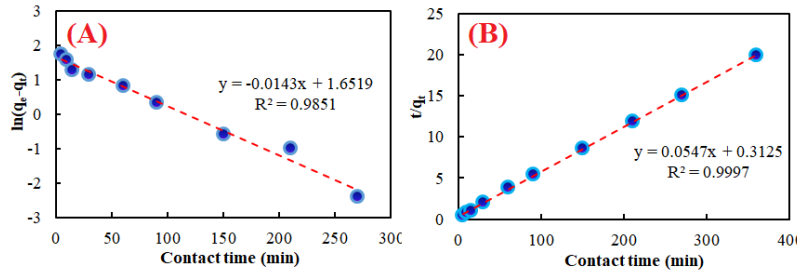

Fig. 5: Adsorption kinetic equation of U(VI) ion by the magnetic Fe_3O_4@Biochar from walnut shell (pseudo-first-order kinetic (A) and pseudo-second-order kinetic (B)).

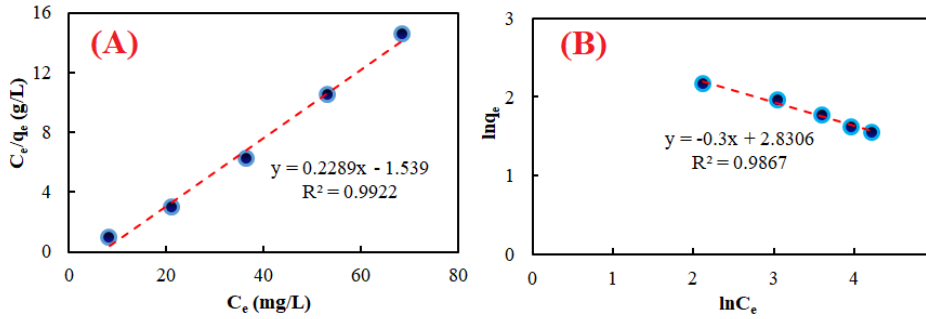

Fig. 6: Adsorption isotherm of U(VI) ion by the magnetic Fe_3O_4@Biochar from walnut shell [Langmuir isotherm (A) and Freundlich isotherm (B)].

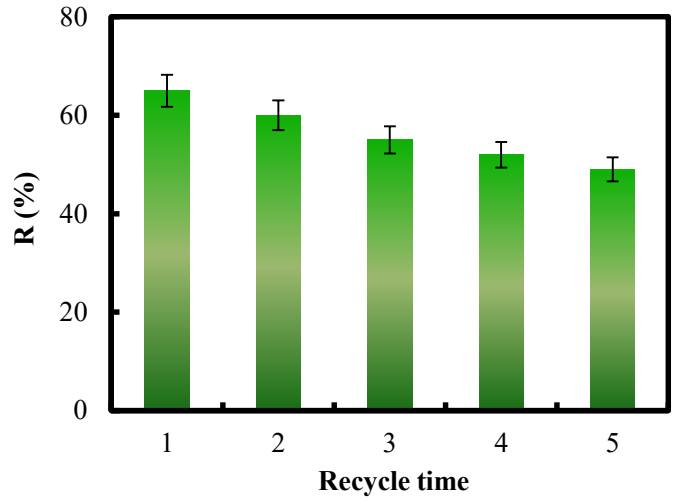

Fig. 7: The repeated reusability of the magnetic Fe_3O_4@Biochar for removal U(VI) ions in solution.

The chemical stability of the magnetic Fe_3O_4@Biochar is good.

CONCLUSION

Biochar is obtained from walnut shells according to the method of pyrolyzed. Additionally, the magnetic Fe_3O_4@Biochar is synthesized. The adsorption of U(VI) ions in solution by the magnetic Fe_3O_4@Biochar is tested. The shape of the magnetic Fe_3O_4@Biochar is fragmented and irregular. There are a large number of functional groups on the surface of the magnetic Fe_3O_4@Biochar, which can facilitate the adsorption of pollutants. The pseudo-first-order kinetic equation and the Langmuir isotherm equation can be fitted for the adsorption of U(VI) in solution by the magnetic Fe_3O_4@Biochar. The maximum adsorption capacity can reach 4.37 $mg.g^{-1}$. The adsorption of the process is chemical adsorption and monolayer adsorption. The chemical stability of the magnetic Fe_3O_4@Biochar is very well.

ACKNOWLEDGEMENTS

This study was financially supported by the project of science and technology plan in Zhejiang Province (LGF20C030001 and LGF21C030001). The authors are very grateful for their support.

REFERENCES

Bhat, S.V., Melo, J.S., Chaugule, B.B. and Souza, S.F.D. 2008. Biosorption characteristics of uranium (VI) from aqueous medium onto Catenella repens, a red alga. J. Hazard. Mater., 158: 628-635.

Chang, K., Li, X., Liao, Q., Hu, B., Hu, J., Sheng, G., Linghu, W., Huang, Y., Asiri, A.M. and Alamry, K.A. 2017. Molecular insights into the role of fulvic acid in cobalt sorption onto graphene oxide and reduced graphene oxide. Chem. Eng. J., 327: 320-327.

Chen, G., Wang, H., Han, L, Yang, N., Hu, B., Qiu, M. and Zhong, X. 2021. Highly efficient removal of U(VI) by novel biochar supported with FeS nanoparticles and chitosan composites. J. Mol. Liq., 327: 114807.

Dai, J., Xu, R.L., Li, W.Y., Yang, Y., Xiao, Y., Mao, H., Qiu, M.Q., Wang, H., Yang, N.C. and Han, L. 2021. Effect of pyrolysis temperature on

adsorption characteristics of biochar derived from corn straw. Nature Environ. Poll. Technol., 20: 291-296.

Das, N. 2012. Remediation of radionuclide pollutants through biosorption-an overview. Clean Soil Air Water, 40: 16-23.

Dong, L., Yang, J., Mou, Y., Sheng, G., Wang, L., Linghu, W., Asiri, A.M. and Alamry, K.A. 2017. Effect of various environmental factors on the adsorption of U (VI) onto biochar derived from rice straw. J. Radioanal. Nucl. Chem., 314: 377-386.

Dutta, D.P. and Nath, S. 2018. Low-cost synthesis of SiO_2/C nanocomposite from corn cobs and its adsorption of uranium(VI), chromium(VI), and cationic dyes from wastewater. J. Mol. Liq., 269: 140-151.

Febrianto, J., Kosasih, A.N., Sunarso, J., Ju, Y.H., Indraswati, N. and Ismadji, S. 2009. Equilibrium and kinetic studies in adsorption of heavy metals using biosorbent: a summary of recent studies. J. Hazard. Mater., 162: 616-645.

Freundlich, H. 1906. Over the adsorption in solution. Z. Phys. Chem., 57: 385-470.

Jang, J., Mirana, W., Divine, S.D., Nawaz, M., Shahzad, A., Woo, S.H. and Lee, D.S. 2018. Rice straw-based biochar beads for the removal of radioactive strontium from aqueous solution. Sci. Total Environ., 615: 698-707.

Han, Y., Cao, X., Ouyang, X., Sohi, S.P. and Chen J. 2016. Adsorption kinetics of magnetic biochar derived from peanut hull on the removal of Cr(VI) from aqueous solution: effects of production conditions and particle size. Chemosphere, 145: 336-341.

Hao, M.J., Qiu, M.Q., Yang, H., Hu, B.W. and Wang, X.X. 2021. Recent advances on preparation and environmental applications of MOF-derived carbons in catalysis. Sci. Total Environ., 760: 143333.

Hu, B.W., Wang, H.F., Liu, R.R. and Qiu M.Q. 2021. Highly efficient U(VI) capture by amidoxime/carbon nitride composites: Evidence of EXAFS and modeling. Chemosphere, 274: 129743.

Langmuir, I. 1918. The adsorption of gases on plane surfaces of glass, mica, and platinum. J. Am. Chem. Soc., 40: 1361-1403.

Li, M.X., Liu, H.B., Chen, T.H., Dong, C. and Sun Y.B. 2019. Synthesis of magnetic biochar composites for enhanced uranium(VI) adsorption. Sci. Total Environ., 651: 1020-1028.

Li, N., Yin, M.L., Tsang, D.C.W., Yang, S.T., Liu, J., Li, X., Song, G. and Wang, J. 2019. Mechanisms of U(VI) removal by biochar derived from Ficus microcarpa aerial root: A comparison between raw and modified biochar. Sci. Total Environ., 697: 134115-134124.

Liu, X.L., Pang, H.W., Liu, X.W., Li, Q., Zhang, N., Mao, L., Qiu, M.Q., Hu, B.W., Yang, H. and Wang, X.K. 2021. Orderly porous covalent organic framework-based materials: superior adsorbents for pollutants removal from aqueous solutions. The Innovations, 2: 100076.

Mellah, A., Chegrouche, S. and Barkat, M. 2006. The removal of uranium(VI) from aqueous solutions onto activated carbon: kinetic and thermodynamic investigations. J. Colloid Interfaces Sci. 296: 434-441.

Mohanty, S.K., Valenca, R., Berger, A., Yu, I.K.M., Xiong, X., Saunders, T. and Tsang, D.C.W. 2018. Plenty of room for carbon on the ground: Potential applications of biochar for stormwater treatment. Sci. Total Environ., 625: 1644-1658.

Qiu, M.Q. and Huang, P. 2017. Kinetic and thermodynamic studies on the adsorption of zinc ions from aqueous solution by the blast furnace slag. Nature Environ. Poll. Technol., 16: 639-642.

Qiu, M.Q., Wang, M., Zhao, Q.Z., Hu, B.W. and Zhu, Y.L. 2018. XANES and EXAFS investigation of uranium incorporation on nZVI in the presence of phosphate. Chemosphere, 201: 764-771.

Qiu, M.Q., Liu, Z.X., Wang, S.Q. and Hu, B.W. 2021. The photocatalytic reduction of U(VI) into U(IV) by ZIF-8/g-C_3N_4 composites at visible light. Environ. Res., 196: 110349.

Sun, Y., Yang, S., Chen, Y., Ding, C., Cheng, W. and Wang, X. 2015. Adsorption and desorption of U(VI) on functionalized graphene oxides: a combined experimental and theoretical study. Environ. Sci. Technol., 49: 4255-4262.

Troyer, L.D., Maillot, F., Wang, Z., Wang, Z., Mehta, V.S., Giammar, D.E. and Catalano, J.G. 2016. Effect of phosphate on U(VI) sorption to montmorillonite: Ternary complexation and precipitation barriers. Geochim. Cosmochim. Acta., 175: 86-99.

Vogel, M., Günther, A., Rossberg, A., Li, B., Bernhard, G. and Raff, J. 2010. Biosorption of U(VI) by the green algae Chlorlla vulgaris in dependence of pH value and cell activity. Sci. Total Environ., 409: 384-395.

Wang, H., Yang, N.C. and Qiu, M.Q. 2020. Adsorption of Cr(VI) from aqueous solution by biochar-clay derived from clay and peanut shell. J. Inor Mater., 35: 301-308.

Wang, H.F., Zhang, Q.Q., Qiu, M.Q. and Hu, B.W. 2021.Synthesis and application of perovskite-based photocatalysts in environmental remediation: A review. J. Mol. Liq., 334: 116029.

Wang, L., Yu, K., Li, J.S., Tsang, D.C.W., Poon, C.S., Yoo, J.C., Baek, K., Ding, S., Hou, D. and Dai, J.G. 2018. Low-carbon and low-alkalinity stabilization/solidification of high-Pb contaminated soil. Chem. Eng. J., 351: 418-427.

Xu, D., Zhao, Y., Sun, K., Gao, B., Wang, Z., Jin, J., Zhang, Z., Wang, S., Yan, Y. and Liu, X. 2014. Cadmium adsorption on plant-and manure-derived biochar and biochar amended sandy soils: Impact of bulk and surface properties. Chemosphere, 111: 320-326.

Yao, L., Yang, H., Chen, Z.S., Qiu, M.Q., Hu, B.W. and Wang, X.X. 2021. Bismuth oxychloride-based materials for the removal of organic pollutants in wastewater. Chemosphere, 273: 128576.

Zhang, M., Gao, B., Varnoosfaderani, S., Hebard, A., Yao, Y. and Inyang, M. 2013. Preparation and characterization of novel magnetic biochar for arsenic removal. Bioresour. Technol., 130: 457-462.